# Finite Element Modelling and Validation of Ultra High Strength Steel Beams

D.Amali[1], P.M.Yuvaranjani[2]
[1]*Assistant Professor, M.E Structural Engineering, Government College of Engineering, Salem.*
[2]*PG Student, Dept. of Civil Engineering, Government College of Engineering, Salem*

***Abstract*- Numerical study of buckling behaviour and flexural strength of plain channel section which is bent about the minor principal axes is given in this journal. Finite element models were modelled and validated against experimental results by using ABAQUS software. The design codes for steel structures cannot be directly used for the ultra-high strength steel (UHSS).**

**Key Words: ultra-high strength steel, plain channel sections, abaqus6.3, 'u' and 'n' orientations.**

## INTRODUCTION

Ultra-high strength steel beams (UHSSB) are structural beams with a yield strength higher than 700 MPa. Ultra-high strength steel that are made from steel alloys which is extremely good for high strength-to-weight ratios. It provides construction of light structures without sacrificing strength, resulting in cost savings and increased design flexibility. The strength of ultra-high strength steels beams allows them to bear heavier loads and it exhibits excellent fatigue and impact resistance, making them suitable for applications subjected to dynamic loads such as cranes and bridges. No codal provision for ultra-high strength steel.

Advantages of ultra-high strength steel beams are

- High strength to weight ratio
- Enhanced load-bearing capacity
- Improved resistance to fatigue and impact
- Reduced material consumption

## LITERATURES

Fangying Wang, Ou Zhao, Ben Young - Flexural behaviour and strengths of press-braked S960 ultra-high strength steel channel section beams.

The experimental study was conducted on eight different UHSS plain channel sections i.e., 20 specimens. Four-point bending tests were performed about the minor principal axes in both the 'u' and 'n' orientations. For flexural members to the examined S960 UHSS channel section beams were evaluated, based on the ultimate moments derived from structural testing and numerical modelling. European code provides overall consistent and precise flexural strength predictions for Class 1 and Class 2 S960 UHSS channel sections in minor-axis bending, but leads to a high level of inaccuracy for the design of their Class 3 and Class 4 counterparts.

Fangying Wang, Lulu zhang, Yating Liang, Ou Zhao- Experimental and numerical studies of press-braked S690 high strength steel channel section beams (2020)

Press – braked S690 high strength steel channel section beams bent about the minor principal axes in both 'u' and 'n' orientation. Accuracy of the flexural strength predicted from various design codes. The European code results in more precise design flexural strengths for beams but less accurate strength for beams , compared to the North American and Australian or New Zealand standards.

Gang Xiong, Yong Feng , Qi peng, Shao-Bo kang, Yue Zhang, Yi-Li fan - Lateral – torsional buckling of 690MPa high strength steel beams (2021)

Eight beams with doubly – symmetric cross section and different height to width ratios were tested under a concentrated point load. It was suggested that GB50017-2003 and GB50017-201X can predict the buckling resistance of Q690 steel beams.

Yufeizhu, Xiang yun, Leroy Gardner - Behaviour and design of high Strength Steel homogeneous and hybrid welded I section beams (2023)

Three-point bending tests on three different welded I sections. Two homogeneous S690 steel welded I

sections. One hybrid welded I sections with S690 steel flanges and an S355 steel web. Test is carried by preventing lateral – torsional buckling. Plastic design can be used for HSS structures, provided the stricter class 1 slenderness limits are employed.

SPECIMEN LABELLING:

The plain channel sections which is shown in the Fangying wang journal paper. The channel section which is bent about minor principal axis in 'u' and 'n' orientations. The cross-section of the channel section is C 100x45x6-mm, where C indicates the channel section. Width of the specimen ($B_f$) x flange width of the specimen ($B_w$) x thickness of the specimen (t). All the dimensions are in mm. R indicates repeated specimen.

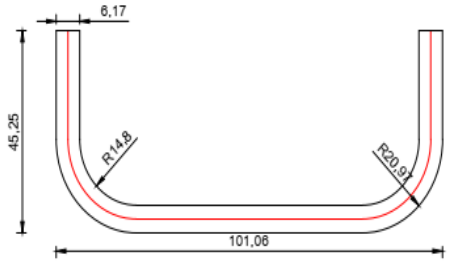


FIGURE 1: u-orientation of C 100x45x6-mm

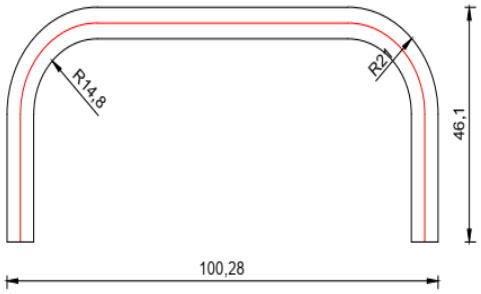


FIGURE 2: n-orientation of C 100x45x6-mm

NUMERICAL VALIDATION:

Abaqus 6.13 is software suitable for finite element analysis. Abaqus CAE (Complete Abaqus Environment) is a software application used for both the modelling and analysis of components and assembling (pre-processing) and visualizing the finite element analysis result. The channel section is bent about minor principal axis i.e., u and n orientations. specimen is simple supported by two steel roller supports, located 50 mm away from the end and loaded at two points. Moment span is 300 mm.

MATERIAL PROPERTIES:

The value of Young's modulus (E) is given as $2x10^5$ $N/mm^2$. The Poisson's ratio is given as 0.3. The yield stress of the material is 985.53 MPa. Density of the material is given as $78.5x10^{-6}$ $N/mm^3$.

PROCESSING STEPS IN ABAQUS

Three common processing steps in ABAQUS are:

1.pre-processing
2.simulation
3.post-processing

Linear analysis (Eigen value buckling analysis)

Steps has assigned in linear perturbation buckle mode.

The transverse load is applied on the loading points as -1.

Then the section is analyzed. Then the Eigen buckling analysis is carried out. In post processing mode, result summary shows the linear analysis load and result the first set was selected and the deformed shape is viewed.

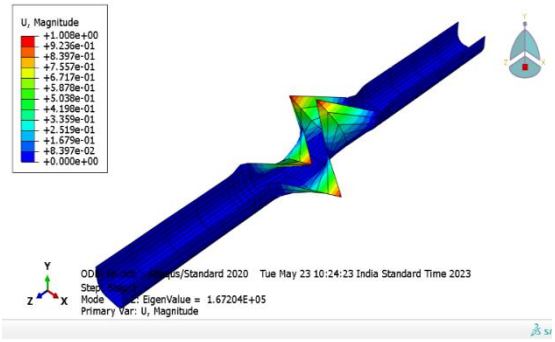


FIGURE 3: Failure mode of C 70x40x6-mm-u during linear analysis

Non-linear buckling analysis

It is more accurate than Eigen value analysis because it employs non-linearity, large deflection, and static analysis to predict buckling loads.

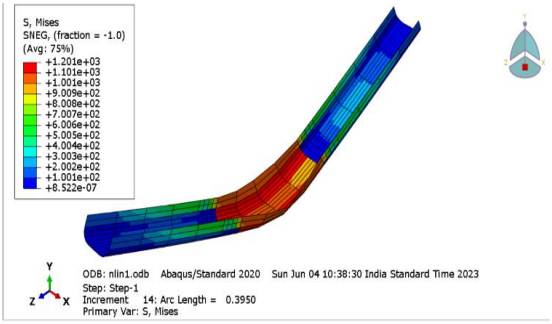


FIGURE 4: Failure mode of C 70x40x6-mm-u during non-linear analysis

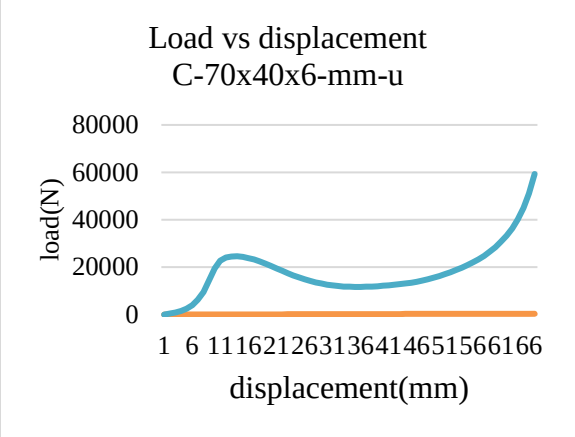


FIGURE 5: Graph of C 70x40x6-mm-u

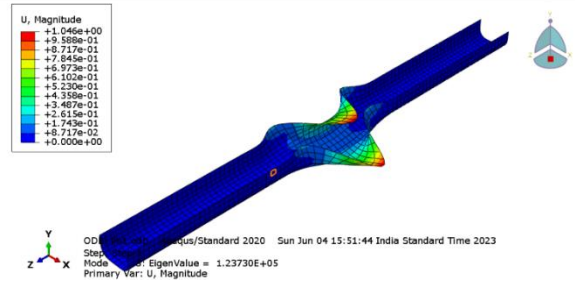


FIGURE 6: Failure mode of C 70x40x6-mm-u(R) during linear analysis

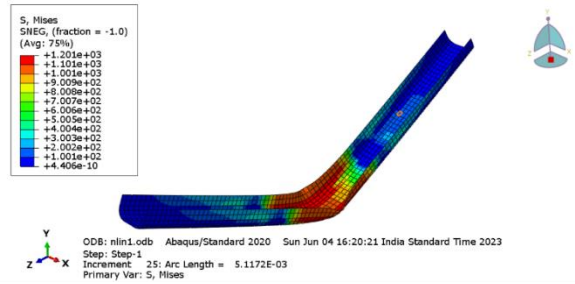


FIGURE 7: Failure mode of C 70x40x6-mm-u(R) during non-linear analysis

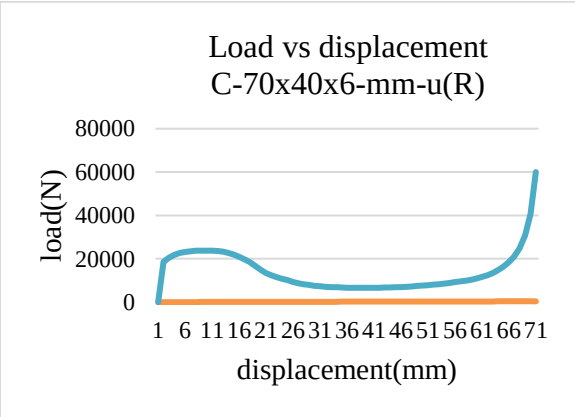


FIGURE 8: Graph of C 70x40x6-mm-u(R)

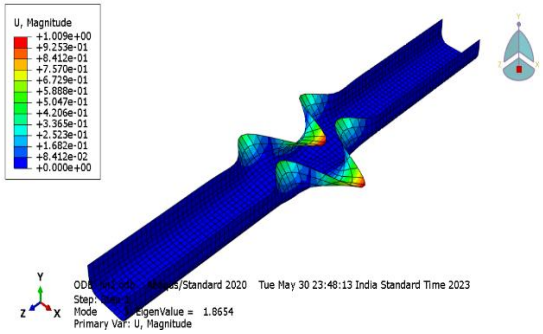


FIGURE 9: Failure mode of C 100x45x6-mm-n during linear analysis

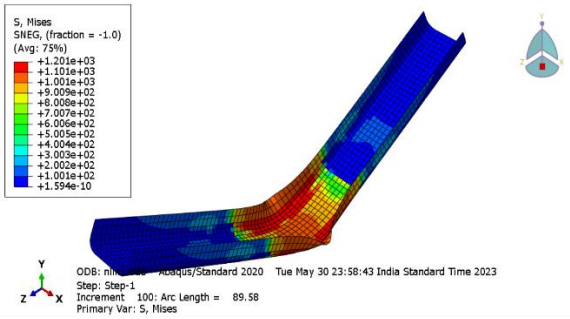


FIGURE 10: Failure mode of C 100x45x6-mm-n during non-linear analysis

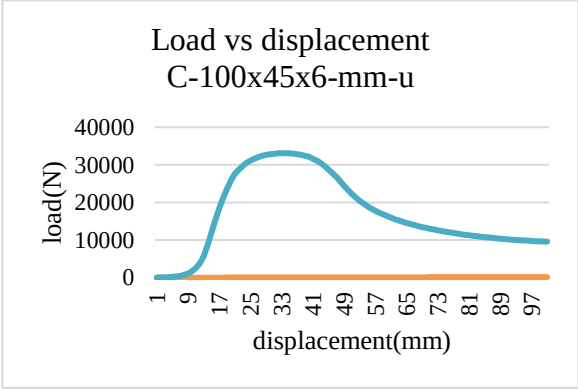


FIGURE 11: Graph of C 100x45x6-mm-u

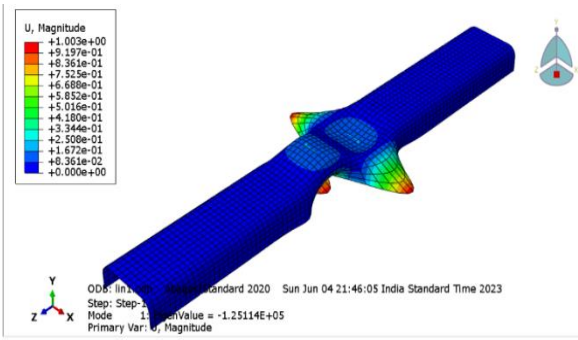


FIGURE 12: Failure mode of C 120x45x6-mm-n during linear analysis

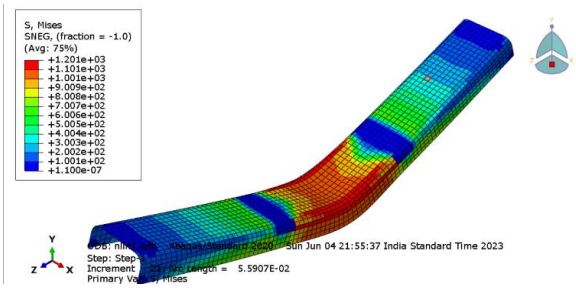


FIGURE 13: Failure mode of C 120x45x6-mm-n during non-linear analysis

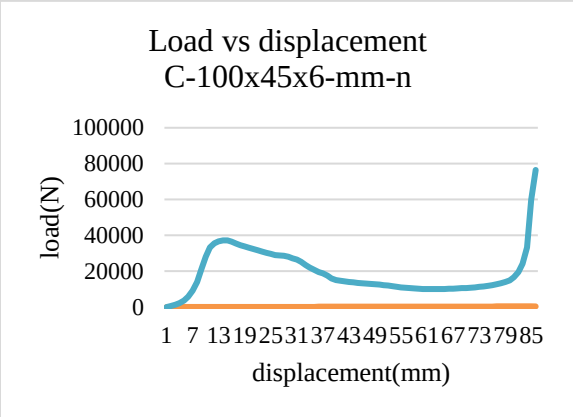


FIGURE 14: Graph of C 120x45x6-mm-n

| s.no | Specimen ID (mm) | $M_{FEM}$ (kN-m) |
|---|---|---|
| 1 | C 70x40x6-u | 8.89 |
| 2 | C 70x40x6-u-R | 8.99 |
| 3 | C 70x40x6-n | 8.50 |
| 4 | C 70x40x6-n-R | 8.82 |
| 5 | C 80x45x6-u | 4.82 |
| 6 | C 80x45x6-n | 9.11 |
| 7 | C 100x45x6-u | 4.96 |
| 8 | C 100x45x6-n | 12.0 |
| 9 | C 120x45x6-u | 5.16 |
| 10 | C 120x45x6-n | 11.47 |
| 11 | C 80x55x6-u | 14.05 |
| 12 | C 80x55x6-n | 7.06 |
| 13 | C 100x60x6-u | 8.91 |
| 14 | C 100x60x6-n | 14.13 |
| 15 | C 120x70x6-u | 21.72 |
| 16 | C 120x70x6-u-R | 10.70 |
| 17 | C 120x70x6-n | 25.78 |
| 18 | C 120x70x6-n-R | 37.15 |

## CONCLUSION

The main objective to obtain in-plane flexural behaviour and constant bending moments with negligible influence from shear. The failure mode of plain is obtained in the moment span of the channel section during linear analysis and non-linear analysis. The numerical moment is validated with the experimental moment.

## REFERENCE

[1] Ma J-L, Chan T-M, Young B. Tests on high-strength steel hollow sections: a review. Pro ICE-Struct Build 2017;170(9):621–30.

[2] Pandey M, Young B. Compression capacities of cold-formed high strength steel tubular T-joints. J Constr Steel Res 2019; 162:105650.

[3] Fang H, Chan T-M. Resistance of axially loaded hot-finished S460 and S690 steel square hollow stub columns at elevated temperatures. Structures 2019; 17:66–73.

[4] Li D, Huang Z, Uy B, Thai HT, Hou C. Slenderness limits for fabricated S960 ultra-high-strength steel and composite columns.
J Constr Steel Res 2019; 159:109–21.

[5] Ma J-L, Chan T-M, Young B. Experimental investigation on stub-column behavior of cold-formed high-strength steel tubular sections. J Struct Eng (ASCE) 2015;142(5):04015174.

[6] Shi G, Ban H, Bijlaard FSK. Tests and numerical study of ultra-high strength steel columns with end restraints. J Constr Steel Res 2012; 70:236–47.

[7] Ban H, Shi G, Shi Y, Bradford MA. Experimental investigation of the overall buckling behaviour of 960MPa high strength steel columns. J Constr Steel Res 2013; 88:256–66.

[8] Ma J-L, Chan T-M, Young B. Experimental investigation of cold-formed high strength steel tubular beams. Eng Struct 2016; 126:200–9.

[9] Rasmussen K. High strength steel structures. Light gauge metal structures recent advances. Springer; 2005. p. 121–41.

[10] Shi G, Zhou W, Lin C. Experimental investigation on the local buckling behavior of 960 MPa high strength steel welded section stub columns. Adv Struct Eng 2015;18(3):423–37.